Renewable Energy 96 (2016) 792–799

Contents lists available at ScienceDirect

Renewable Energy

journal homepage: www.elsevier.com/locate/renene

Sun-tracking imaging system for intra-hour DNI forecasts

Yinghao Chu, Mengying Li, Carlos F.M. Coimbra*

Department of Mechanical and Aerospace Engineering, Jacobs School of Engineering, Center of Excellence in Renewable Resource Integration and Center for Energy Research, University of California in San Diego, 9500 Gilman Drive, La Jolla, CA 92093, USA

ARTICLE INFO

Article history:
Received 20 January 2016
Received in revised form
10 April 2016
Accepted 11 May 2016

Keywords:
Sun-tracking
Solar forecasting
Sky imaging
Stochastic learning

ABSTRACT

A Sun-tracking imaging system is implemented for minimizing circumsolar image distortion for improved short-term solar irradiance forecasts. This sky-imaging system consists of a fisheye digital camera mounted on an automatic solar tracker that follows the diurnal pattern of the Sun. The Sun is located at the geometric center of the sky images where the fisheye distortion is minimized. Images from this new system provide more information about the circumsolar sky cover, which provides critical information for intra-hour solar forecasts, particularly for direct normal irradiance. An automatic masking algorithm has been developed to separate the sky area from ground obstacles and the image edges for each image that is collected. Then numerical image features are extracted from the segmented sky area and are used as exogenous inputs to MultiLayer Perceptron (MLP) models for direct normal irradiance forecasts. Sixty-seven days of irradiance and image measurements are used to train, optimize, and assess the MLP-based forecast models for solar irradiance. The results show that the MLP forecasts based on the newly proposed sky-imaging system significantly outperform the reference models in terms of statistical metrics and forecast skill, particularly for shorter horizons, achieving forecast skills 18%–50% higher than the skills of a reference MLP-based model that is based on a zenith-pointed, stationary sky-imaging system.

1. Introduction

The market penetration of solar power generation is growing rapidly and this growth imposes challenges to the operations of electric power grids [1,2], which need to be balanced in real time [3]. Ground-level solar irradiance is highly variable due to atmospheric process, especially cloud cover and aerosol content. The variability of irradiance at ground level affects the reliability of solar power generation [4], which in turn compromises the stability and integration costs for high solar penetration grids [5]. Accurate solar irradiance and power forecasts are enabling technologies that have the potential to mitigate the uncertainty of solar power generation and to optimize demand and storage solutions [1,6–10].

Effective solar forecasting methods have been developed for various temporal horizons, ranging from several minutes to a few days. Commonly employed methods include regressive or stochastic learning models [4,11–21] and physical models based on remote-sensing or local-sensing techniques [7,19,20,22–27]. For intra-hour forecasts, advanced hybrid models that integrate stochastic learning and local sensing techniques have been developed in the recent years [3,19,20,28]. When assessed in real time, the hybrid models achieve forecast skills ranging from 6% to 32% over reference persistence models [1,28,29].

To date, local-sensing systems are mostly based on sky imagers or fisheye cameras [27]. The lenses of these imagers are stationary and typically zenith-oriented. In this work, a sky-imaging system consisting of a low-cost fisheye camera mounted on an automatic solar tracker is used. The lens of this proposed system tracks the trajectory of the Sun and provides sky images centered at the apparent position of the Sun in the sky. In comparison to whole sky images from stationary imagers, Sun-centered sky images provide more information about the circumsolar sky-cover with substantially less distortion. Therefore, this new sky-imaging system has high potential to further enhance the performance of intra-hour Direct Normal Irradiance (DNI) forecasts.

In general, sky images capture not only the sky area but also the ground obstacles and darken image edges (shown in Figs. 2–7). For stationary imaging systems, manually-annotated masks are commonly used to obtain the sky area and to discard the other areas that are not useful to solar forecasts [27,30]. However, in the

---

* Corresponding author.
E-mail address: ccoimbra@ucsd.edu (C.F.M. Coimbra).

http://dx.doi.org/10.1016/j.renene.2016.05.041

new sky-imaging system presented here, each image captured requires a specific mask because the camera is non-stationary. Generating manually-annotated mask for each sky image is not practical for automatic real-time forecasts. Therefore, a smart masking algorithm has been developed to automatically analyze the color gradients of an image and to segment the sky area from the other, less-informative areas. Once the sky area is identified using the automatic masking algorithm, image features are extracted from the sky area and are used as exogenous inputs to a stochastic-learning model (MultiLayer Perception (MLP) in this work) to forecast intra-hour DNI.

We describe the new sky-imaging system in Section 2. The automatic masking algorithm and DNI forecasting model are presented in Section 3. The statistic metrics used to assess the DNI forecasts are also presented in this section. Operational results are presented in Section 4, and conclusions are presented in Section 5.

2. Data

A Multi-Filter Rotating Shadowband Radiometer (MFR-7, manufactured by Yankee Environmental Systems) has been installed at University of California San Diego (latitude = 32.881°, longitude = −117.238°) to measure the DNI components of broadband solar irradiance. The DNI data are sampled every minute and are logged using a Campbell Scientific (CR1000) data logger. Two Vivotek fisheye cameras (model FE8171V) have been installed close to the MFR-7. These cameras collect 8-bit RGB sky images (1536 × 1536 pixels) using 3.1 MP CMOS sensors and a 360° panoramic-view lens. One camera has been installed in a stationary position with its lens pointing to the zenith. This stationary camera (named SkyCam) captures whole-sky images centered at the zenith. The other camera (named SunCam) is mounted on an Eppley automatic solar tracker that points the camera lens toward the apparent position of the Sun. A photo of the employed Sun-centered devices is presented in Fig. 1. The captured images (see sample images in Figs. 6 and 7) are transferred via FTP to a UCSD server once per minute. The DNI data and the sky images are stored in a MySQL database. DNI measurements and sky images with the same time label are grouped as data instances.

The analysis of this work uses 44,393 data instances (from June 20, 2013 to August 25, 2013; nighttime measurements have been discarded). The first 30,000 data instances (from June 20, 2013 to August 03, 2013) are assigned as a training set for model training and optimization. The remaining 14,393 data instances (Aug 03, 2013 to Aug 25, 2013) are assigned as a testing set to assess the performance of the forecasting models. Both the training and testing sets include the diverse conditions of weather and cloud content.

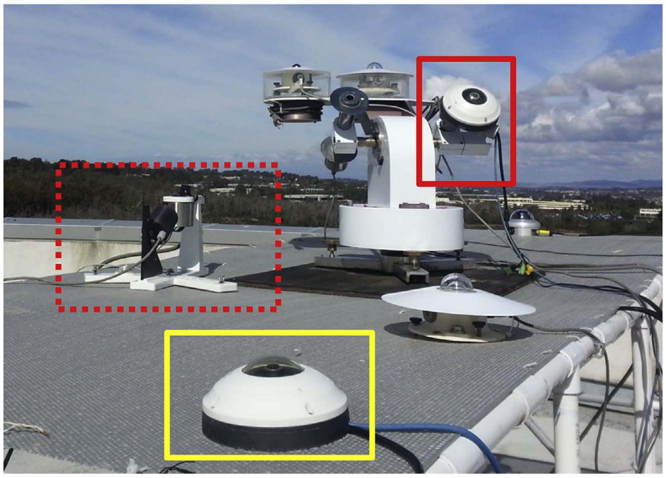

Fig. 1. Photo of the employed MFR-7 (quoted with red dash square), SkyCam (quoted with yellow square), and the SunCam (quoted with red square). (For interpretation of the references to color in this figure legend, the reader is referred to the web version of this article.)

The MFR-7 is a first-class radiometer that meets the accuracy requirements of this work. The fisheye lenses of both the SkyCam and the SunCam are regularly cleaned to maintain satisfactory image quality. Images with excessive amounts of dust are manually discarded. In addition, the analysis of this work uses data instances when the solar elevation angle is higher than 15° to reduce the effect of ground obstacles (e.g. trees, buildings).

3. Methods

3.1. Automatic masking algorithm

SunCam moves to track the diurnal pattern of the Sun. Therefore, automatic masking algorithm has been developed to segment the sky area from obstacles and image edge for each SunCam image. The algorithm is suitable for images from both SkyCam and SunCam, making it a universal algorithm. The automatic masking algorithm initiates with a Sun locating algorithm.

3.1.1. Sun locating algorithm

The Sun locating algorithm considers seven features of a sky image: Red (R), Green (G), Blue (B), Hue (H), Saturation (S), Value (V) and Intensity (I). The features are all normalized to 0–1 range. As shown in Fig. 2, the Hue and Saturation of Sun area are relatively small while the Red, Green, Blue, Value and Intensity are relatively large. Therefore, image features F_8 is introduced, which is defined as:

$$F_8 = \text{logical}\left(\frac{R+G+B+V+I}{5} - \frac{H+S}{2} > \theta_e\right), \tag{1}$$

where θ_e is a threshold which is set to 0.85 empirically. As shown in Fig. 3(b), only pixels in the circumsolar region have non-zero F_8.

The following process is used to eliminate the outsiders shown in Fig. 3(b): First define [*#rows*, *#cols*] as the locations of non-zero elements of F_8; Then define [*#rows**, *#cols**] as the locations of non-zero elements within one standard derivation of all [*#rows*, *#cols*]; finally the Sun location in an image is calculated as:

$$\text{SunL} = [\text{mean}(\#rows*),\ \text{mean}(\#cols*)]. \tag{2}$$

Fig. 3(c) shows the algorithm finds the location of the Sun successfully.

3.1.2. Masking algorithm

As shown in Fig. 2, the Red, Blue, Green, Value and Intensity features of obstacles are smaller than that of sky. Therefore, a feature vector is defined to differentiate sky area from obstacles:

$$\vec{F} = [R, G, B, V, I]. \tag{3}$$

The gradient of feature vector $\vec{F}$ is calculated to find the edges of obstacles (Fig. 3(d)),

$$\nabla\vec{F} = \frac{d\vec{F}}{d\vec{x}} = \sum_{i=1}^{5}\sqrt{\left(\frac{dF_i}{dx}\right)^2 + \left(\frac{dF_i}{dy}\right)^2}. \tag{4}$$

The edges are,